PHYSICAL REVIEW B VOLUME 54, NUMBER 20 15 NOVEMBER 1996-II

# Theory of surface and interface transverse elastic waves in $N$-layer superlattices

E. H. El Boudouti
*Laboratoire de Dynamique et Structure des Matériaux Moleculaires, Centre National de la Recherche Scientifique (URA 801), Université des Sciences et Technologies de Lille, UFR de Physique, F-59655 Villeneuve d'Ascq Cedex, France and Département de Physique, Faculté des Sciences, Oujda, Morocco*

B. Djafari-Rouhani, A. Akjouj, and L. Dobrzynski
*Laboratoire de Dynamique et Structure des Matériaux Moleculaires, Centre National de la Recherche Scientifique (URA 801), Université des Sciences et Technologies de Lille, UFR de Physique, F-59655 Villeneuve d'Ascq Cedex, France*

(Received 1 July 1996)

$N$-layer superlattices are formed out of a periodic repetition of $N$ different slabs. Such materials for $N=3$ and 4 are now easily grown by molecular-beam epitaxy. We present closed form expressions for localized and resonant transverse elastic waves associated with the surface of a semi-infinite $N$-layer superlattice, with or without a cap layer, and in contact either with vacuum or with a homogeneous substrate. We also calculate the corresponding Green's- function and densities of states. These general results are illustrated by a few applications to four-layer superlattices made of Nb-Fe-Nb-Cu and Nb-Cu-Nb-Cu. We show that increasing the number of the layers in each unit cell of the superlattice increases, in general, the number of the minigaps and surface modes. We generalize some of the results obtained previously in the case of two-layer superlattices, namely, (i) the creation from an infinite superlattice of a free surface gives rise to $\delta$ peaks of weight $(-\frac{1}{4})$ in the density of states, at the edges of the superlattice bulk bands; (ii) by considering together the two complementary semi-infinite superlattices obtained by cleavage of an infinite superlattice along a plane parallel to the interfaces, one always has as many localized surface modes as minigaps, for any value of the wave vector $\mathbf{k}_{\parallel}$ (parallel to the interfaces). Finally, we investigate the localized and resonant modes associated with the presence of a cap layer on top of the superlattice. [S0163-1829(96)00944-7]

## I. INTRODUCTION

The growth of $N$-layered superlattices for $N \geqslant 3$ became standard in the last decade. Investigations of the physical properties of such polytype superlattices attract increasing interest connected with the search of more performant new materials for microelectronics, see, for example, Refs. 1–3 and references therein. The idea of polytype three-layer superlattices was proposed first[4] together with an application to InAs-GaSb-AlSb multiheterojunctions. Many theoretical and experimental investigations appeared since dealing with nearly free electrons,[5–14] elastic transverse waves,[8,15–22] and polaritons.[8,23–25]

The theories for all these waves are isomorphic.[8,9] A general dispersion relation for all these excitations in bulk $N$-layered superlattices was given before.[8] Almost all the above cited papers rederive this dispersion relation for $N=3$ or 4 and even[10] for $N=6$. A few papers[9,11,14,22] address this question for any value of $N$ with different recursive methods but without reaching the explicit expression given in Ref. 8. Let us also cite studies of spin waves in $N$-layered superlattices.[26] There are also several experimental Raman studies of folded acoustic modes in periodic superlattices with $N>2$ constituents,[15–18] as well as in quasiperiodic superlattices,[27–29] based on the Fibonacci sequence, approximated by periodic superlattices with $N>2$.

The object of this paper is to investigate the transverse elastic waves in semi-infinite $N$-layer superlattices. The superlattice which may possibly be covered by a cap layer is in contact either with vacuum or with a substrate. Following Ref. 8 dealing with infinite $N$-layer superlattices, a main result of this work will be to give explicit dispersion relations for surface and interface waves in semi-infinite superlattices which can be used by any reader interested by the subject without going into a detailed calculation. Such expressions can actually be derived by using either the transfer matrix or the Green-function methods. In order to also investigate other vibrational properties of semi-infinite superlattices such as the local and total densities of states, and therefore the spatial distribution of the states and, in particular, the possibility of resonant (or leaky) waves, we present in this paper explicit expressions of the Green function in these heterostructures. The simpler method of transfer matrix will be very briefly referred to in the appendix. Although our attention will be focused in this work on transverse elastic waves in superlattices, our calculation can simply be transposed by standard mathematical isomorphism for studying electrons or polaritons in these systems.

The organization of this paper is as follows. Section II deals with the infinite $N$-layer superlattice and Sec. III with a capped semi-infinite superlattice in contact with an homogenous substrate. The particular limits of a free surface with or without a cap layer and of an interface between an uncapped superlattice and a substrate will also be outlined from the above general case. In Sec. IV, we illustrate these general results by analytical and numerical applications to surface and interface waves in four-layer superlattices with emphasis on the existence and localization properties of surface modes and on the increase of their number with the number of layers in each unit cell of the superlattice. The main conclusions are summarized in Sec. V.

0163-1829/96/54(20)/14728(14)/$10.00  

## II. THE INFINITE $N$-LAYER SUPERLATTICE

The $N$-layer superlattice is formed out of an infinite repetition of a unit cell labeled by the index $n$ and containing $N$ different slabs. Each of these slabs labeled $i$ ($1\leqslant i\leqslant N$) is characterized by its elastic constants $C^{(i)}_{\alpha\beta}$, its mass density $\rho_i$, and a width $d_i$. All of the interfaces are taken to be parallel to the $(x_1,x_2)$ plane. A space position along the $x_3$ axis in medium $i$ belonging to the unit cell $n$ is indicated by $(n,i,x_3)$, where $-d_i/2\leqslant x_3\leqslant d_i/2$. The period of the superlattice is called

$$D=\sum_{i=1}^{N} d_i . \tag{1}$$

Due to the symmetry of translation parallel to the $(x_1,x_2)$ plane, one can define a wave vector $\mathbf{k}_\parallel$ parallel to the interfaces and reduce the whole problem to a one-dimensional problem, function of $\mathbf{k}_\parallel$. In the infinite superlattice, one can also define a wave vector $k_3$ along the axis of the superlattice associated with the period $D$.

In this paper, we limit ourselves to the case of shear horizontal vibrations where the displacement field $\mathbf{u}$ is along the $x_2$ axis and the wave vector $\mathbf{k}_\parallel$ is directed parallel to the $x_1$ axis. Then (see below), one can consider with the same general equations the case of a superlattice built of isotropic materials, or built of hexagonal crystals with (0001) (isotropic) interfaces, or of cubic crystals with (001) interfaces and $\mathbf{k}_\parallel$ along the [100] crystallographic direction.

Let us first recall that, in all the above cases, the displacement field $u_2$ in an infinite homogeneous material $i$ satisfies the equation[30]

$$\frac{F_i}{\alpha_i}\left[\frac{\partial^2}{\partial x_3^2}-\alpha_i^2\right]u_2(\mathbf{k}_\parallel;x_3)=0, \tag{2}$$

where

$$F_i=\alpha_i C^{(i)}_{44}, \tag{3a}$$

and $\alpha_i$ is defined as

$$\alpha_i^2=k_\parallel^2-\rho_i\,\frac{\omega^2}{C^{(i)}_{44}}, \tag{3b}$$

where $\omega$ is the frequency of the vibrations, if the material $i$ is isotropic or of cubic symmetry ($\mathbf{k}_\parallel$ being along the [100] direction), or as

$$\alpha_i^2=k_\parallel^2\left(\frac{C^{(i)}_{11}-C^{(i)}_{12}}{2C^{(i)}_{44}}\right)-\rho_i\,\frac{\omega^2}{C^{(i)}_{44}}, \tag{3c}$$

if the medium $i$ is of hexagonal symmetry.

Now, the Green's function of the infinite homogeneous medium $i$ associated with the displacement field $u_2$ satisfies the following equation;

$$\frac{F_i}{\alpha_i}\left[\frac{\partial^2}{\partial x_3^2}-\alpha_i^2\right]G_i(\mathbf{k}_\parallel;x_3,x_3')=\delta(x_3-x_3'), \tag{4a}$$

and can be expressed as

$$G_i(\mathbf{k}_\parallel;x_3,x_3')=-\frac{1}{2F_i}\,e^{-\alpha_i|x_3-x_3'|}. \tag{4b}$$

We would briefly recall the principle for building the Green function of the infinite and semi-infinite superlattice.[30] This will enable us to present the dispersion relations of the surface and interface waves in the superlattice as well as the expressions for the local and the total densities of states without going into the details of this calculation. Our calculation is based on the theory of interface response in composite materials[9] in which the Green function $\mathbf{g}$ of a composite system is given as

$$\mathbf{g}(\mathbf{DD})=\mathbf{G}(\mathbf{DD})-\mathbf{G}(\mathbf{D}M)\mathbf{G}^{-1}(MM)\mathbf{G}(M\mathbf{D}) +\mathbf{G}(\mathbf{D}M)\mathbf{G}^{-1}(MM)\mathbf{g}(MM)\mathbf{G}^{-1}(MM)\mathbf{G}(M\mathbf{D}), \tag{5}$$

where $\mathbf{D}$ and $M$ are, respectively, the whole space and the space of the interfaces in the composite materials; $G$ is a block-diagonal matrix in which each block $G_i$ corresponds to the bulk Green function of the subsystem $i$ [Eq. (4)]. In our case, the superlattice is composed of slabs of materials $i=1,\ldots,N$. In Eq. (5), the calculation of $\mathbf{g}(\mathbf{DD})$ requires, besides $G_i$, the knowledge of $\mathbf{g}(MM)$. The latter can be obtained, in practice, by inverting the matrix $\mathbf{g}^{-1}(MM)$ which can be simply built[9] from a juxtaposition of the matrices $\mathbf{g}_{si}^{-1}(MM)$, where $\mathbf{g}_{si}(MM)$ is the interface Green's function of the slab $i$ alone with stress-free boundary conditions.

Therefore the first step before addressing the problem of layered materials will be to know the surface elements of the Green's function $\mathbf{g}_{si}$ of a slab of medium $i$, such that $-d_i/2\leqslant x_3\leqslant d_i/2$, with stress-free boundary conditions. These surface elements can be written[9] in the form of a $(2\times2)$ matrix $\mathbf{g}_{si}(M_iM_i)$, within the interface space $M_i\equiv\{-d_i/2,d_i/2\}$. The inverse of this matrix has the following form:

$$[\mathbf{g}_{si}(M_i,M_i)]^{-1}=\begin{pmatrix} A_i & B_i \\ B_i & A_i\end{pmatrix}, \tag{6}$$

where

$$A_i=-(F_iC_i)/S_i, \tag{7a}$$

$$B_i=F_i/S_i, \tag{7b}$$

$$C_i=\cosh(\alpha_i d_i), \tag{7c}$$

and

$$S_i=\sinh(\alpha_i d_i). \tag{7d}$$

Within the total interface space of the $N$-layered superlattice, the inverse of the matrix giving all the interface elements of the Green's function $\mathbf{g}$ of this superlattice is an infinite tridiagonal matrix[9] formed by linear superposition of the elements of the $[\mathbf{g}_{si}(M_i,M_i)]^{-1}$.

Taking advantage of the periodicity $D$ in the direction $x_3$ of the $N$-layered superlattice, the Fourier transformed $[\mathbf{g}(k_3;M,M)]^{-1}$ of the above infinite tridiagonal matrix within one unit cell ($1\leqslant i\leqslant N$) has the following form:

$$[\mathbf{g}(k_3;MM)]^{-1}=\begin{bmatrix} A_N+A_1 & B_1 & & & & & B_N e^{-ik_3D} \\ B_1 & A_1+A_2 & B_2 & & & & \\ & B_2 & A_2+A_3 & \ddots & & & \\ & & & & A_{N-3}+A_{N-2} & B_{N-2} & \\ & & & & B_{N-2} & A_{N-2}+A_{N-1} & B_{N-1} \\ B_N e^{ik_3D} & & & & & B_{N-1} & A_{N-1}+A_N \end{bmatrix}. \tag{8}$$

Thanks to the simple form of this matrix, it is possible to calculate its inverse in closed form, as a function of the following sums which are the elements of a transfer matrix as shown in the Appendix.

$$(T_{11})_{1,\ldots,N}=\sum_{\{i_1,\ldots,i_p\}\{i_{p+1},\ldots,i_N\}} C_{i_1}C_{i_2}\ldots C_{i_p}S_{i_{p+1}}S_{i_{p+2}}\ldots S_{i_N}\frac{F_{i_N}}{F_{i_{N-1}}}\frac{F_{i_{N-2}}}{F_{i_{N-3}}}\cdots\frac{F_{i_{p+2}}}{F_{i_{p+1}}}, \tag{9a}$$

$$(T_{22})_{1,\ldots,N}=\sum_{\{i_1,\ldots,i_p\}\{i_{p+1},\ldots,i_N\}} C_{i_1}C_{i_2}\ldots C_{i_p}S_{i_{p+1}}S_{i_{p+2}}\ldots S_{i_N}\frac{F_{i_{N-1}}}{F_{i_N}}\frac{F_{i_{N-3}}}{F_{i_{N-2}}}\cdots\frac{F_{i_{p+1}}}{F_{i_{p+2}}}, \tag{9b}$$

$$(T_{21})_{1,\ldots,N}=\sum_{\{i_1,\ldots,i_p\}\{i_{p+1},\ldots,i_N\}} C_{i_1}C_{i_2}\ldots C_{i_p}S_{i_{p+1}}S_{i_{p+2}}\ldots S_{i_N}\frac{F_{i_N}}{F_{i_{N-1}}}\frac{F_{i_{N-2}}}{F_{i_{N-3}}}\cdots\frac{F_{i_{p+3}}}{F_{i_{p+2}}}F_{i_{p+1}}, \tag{9c}$$

$$(T_{12})_{1,\ldots,N}=\sum_{\{i_1,\ldots,i_p\}\{i_{p+1},\ldots,i_N\}} C_{i_1}C_{i_2}\ldots C_{i_p}S_{i_{p+1}}S_{i_{p+2}}\ldots S_{i_N}\frac{F_{i_{N-1}}}{F_{i_N}}\frac{F_{i_{N-3}}}{F_{i_{N-2}}}\cdots\frac{F_{i_{p+2}}}{F_{i_{p+3}}}\frac{1}{F_{i_{p+1}}}, \tag{9d}$$

The numbers in these suites are in decreasing order and the suite of terms $(i_{p+1},\ldots,i_N)$ has to be even in Eqs. (9a) and (9b) and odd in Eqs. (9c) and (9d). The first term in the summation in Eqs. (9a) and (9b) (corresponding to $p=N$) should be understood as $C_1, C_2 \ldots C_N$. Each summation provides $2^{N-1}$ different terms adding one to each other.

The bulk bands of the $N$-layer superlattice are easily obtained from the determinant of the matrix given by Eq. (8) in the following form:

$$\cos(k_3D)=\xi, \tag{10}$$

where

$$\xi=\frac{1}{2}[(T_{11})_{1,\ldots,N}+(T_{22})_{1,\ldots,N}]. \tag{11}$$

It is also straightforward to Fourier analyze back into real space all the elements of $\mathbf{g}(k_3;MM)$ and obtain all the interface elements of $\mathbf{g}$, in the following form:

$$g\left(n,i,-\frac{d_i}{2};n',j,-\frac{d_j}{2}\right)=\begin{cases}(T_{12})_{i,\ldots,N,1,\ldots,i-1}\dfrac{t^{|n-n'|+1}}{t^2-1}, & i=j\\ (T_{12})_{j,\ldots,N,1,\ldots,i-1}\dfrac{t^{|n-n'|+1}}{t^2-1}+(T_{12})_{i,\ldots,j-1}\dfrac{t^{|n-n'-1|+1}}{t^2-1}, & i<j\leqslant N\\ (T_{12})_{i,\ldots,N,1,\ldots,j-1}\dfrac{t^{|n-n'|+1}}{t^2-1}+(T_{12})_{j,\ldots,i-1}\dfrac{t^{|n-n'+1|+1}}{t^2-1}, & j<i\leqslant N.\end{cases} \tag{12}$$

Here the different $(T_{12})$ are obtained from Eq. (9d) with due account for the indices giving the order of the layers beginning from the first and ending by the last and

$$t=\begin{cases}\xi+(\xi^2-1)^{1/2}, & \xi<-1\\ \xi\pm i(1-\xi^2)^{1/2}, & -1<\xi<+1\\ \xi-(\xi^2-1)^{1/2}, & \xi>1.\end{cases} \tag{13}$$

Inside the bulk bands of the superlattice $(-1<\xi<1)$, the sign in the expression for $t$ has to be chosen such that $|t(\omega^2+i\epsilon)|_{\epsilon\to 0}$ will be slightly smaller than one.

The expression of the Green's function between any two points of the infinite superlattice can easily be derived from Eq. (5),

$$g(n,i,x_3;n',i',x_3')=\delta_{nn'}\delta_{ii'}U_i(x_3,x_3')+\frac{1}{S_iS_i'}\times\left\{\sinh\left[\alpha_i\left(\frac{d_i}{2}-x_3\right)\right];\right.\times\left.\sinh\left[\alpha_i\left(\frac{d_i}{2}+x_3\right)\right]\right\}\mathbf{g}(M_m,M_{m'})\times\left\{\begin{array}{c}\sinh\left[\alpha_{i'}\left(\dfrac{d_{i'}}{2}-x_3'\right)\right]\\ \sinh\left[\alpha_{i'}\left(\dfrac{d_{i'}}{2}+x_3'\right)\right]\end{array}\right\}, \tag{14}$$

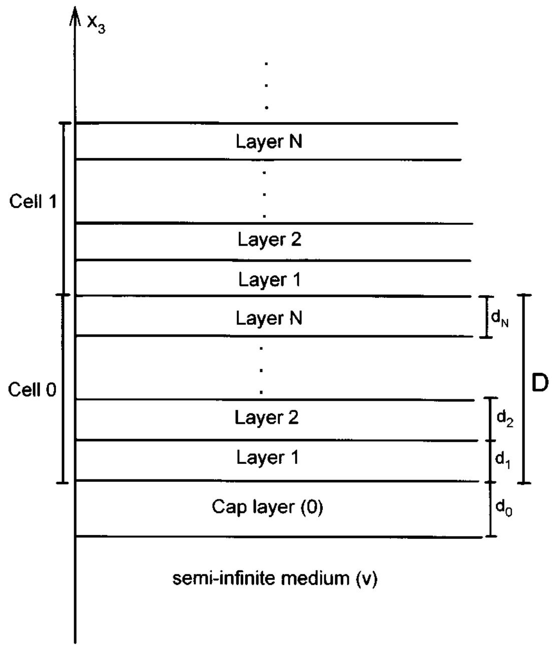


FIG. 1. Schematic representation of a capped semi-infinite $N$-layer superlattice in contact with an homogeneous substrate. $d_0, d_1, d_2, \ldots, d_N$, respectively, are the thicknesses of the cap layer and of the $N$ different slabs out of which the unit cell of the superlattice is built. $D$ is the period of the superlattice.

where

$$U_i(x_3,x_3') = -\frac{1}{2F_i}\exp[-\alpha_i|x_3-x_3'|] + \frac{1}{2F_iS_i}$$
$$\times\left\{\sinh\left[\alpha_i\left(\frac{d_i}{2}-x_3'\right)\right]\exp\left[-\alpha_i\left(\frac{d_i}{2}+x_3\right)\right]\right.$$
$$\left.+\sinh\left[\alpha_i\left(\frac{d_i}{2}+x_3'\right)\right]\exp\left[-\alpha_i\left(\frac{d_i}{2}-x_3\right)\right]\right\}. \qquad (15)$$

In Eq. (14) the last three terms are the product of a $(1\times2)$ matrix by the $(2\times2)$ $g(M_m,M_{m'})$ matrix and by a $(2\times1)$ matrix. $g(M_m,M_{m'})$ is the $(2\times2)$ matrix formed out of the elements given by Eq. (12), for $m\equiv(n,i,\pm d_i/2)$ and $m'\equiv(n',i',\pm d_i'/2)$.

The knowledge of the above results, enable us to address now the problem of a capped surface of such a superlattice in contact with an homogenous semi-infinite substrate.

## III. THE CAPPED SURFACE AND THE INTERFACE

In this section, we will first outline the derivation of the Green's function and then give the results for the surface states and the density of states.

### A. The Green's function

In order to obtain the physical properties of a semi-infinite $N$-layer superlattice terminated by a capped surface in contact with a semi-infinite homogeneous medium (Fig. 1), it is convenient to consider the following three steps:

(i) The semi-infinite superlattice, with a stress-free surface terminated by the layer $(n=0,\ i=1)$, is obtained by removing the $(n=-1,\ i=N)$layer out of the infinite $N$-layer superlattice. The corresponding $[\mathbf{g}_s(M_s,M_s)]^{-1}$ in the $M_s$ semi-infinite interface space $(n\geqslant0,\ i=1,\ldots,N)$, is represented by a semi-infinite tridiagonal matrix whose surface diagonal element situated at $(n=0,\ i=1,\ -d_1/2)$ is equal to $A_1$.

(ii) We consider a semi-infinite homogeneous medium characterized by the parameters $\alpha_v$, $F_v$ [Eq. (3)] and capped by a layer characterized by the parameters $\alpha_0$, $F_0$ [Eq. (3)] and by $C_0$ and $S_0$ [Eq. (7)].

Within the interface space $M_0=(-1,0,\pm d_0/2)$, of this system, one obtains[9]

$$[\mathbf{g}_{s0}(M_0,M_0)]^{-1} = \begin{pmatrix} A_0-F_v & B_0 \\ B_0 & A_0 \end{pmatrix}. \qquad (16)$$

By inversion of this matrix, one gets

$$g_{s0}^{-1}\left(-1,0,\frac{d_0}{2};-1,0,\frac{d_0}{2}\right) = -RF_v. \qquad (17)$$

where

$$R = \frac{1+\dfrac{F_0S_0}{F_vC_0}}{1+\dfrac{F_vS_0}{F_0C_0}}. \qquad (18)$$

(iii) The above semi-infinite superlattice is coupled to the cap layer 0 deposited on the substrate $v$. The Green's function of this final system in the interface space has as its inverse $\mathbf{d}^{-1}(M_s,M_s)$ a semi-infinite triadiagonal matrix. The surface diagonal element of this matrix situated at $(n=0,\ i=1,\ -d_1/2)$ is equal to $(A_1-RF_v)$. By standard diagonalization[9] of such a semi-infinite tridiagonal matrix, one obtains for $n,n'\geqslant0$ and $i,j=1,\ldots,N$:

$$d\left(n,i,-\frac{d_i}{2};n',j,-\frac{d_j}{2}\right) = g\left(n,i,-\frac{d_i}{2};n',j,-\frac{d_j}{2}\right)$$
$$-\frac{t^{n+n'+1}}{t^2-1}\frac{Y_iY_j}{W}, \qquad (19)$$

where

$$W=(RF_v)^2(T_{12})_{1,\ldots,N}+RF_v[(T_{11})_{1,\ldots,N}-(T_{22})_{1,\ldots,N}]$$
$$-(T_{21})_{1,\ldots,N}, \qquad (20)$$

and the $Y_i$ take the form

$$Y_1=-RF_v(T_{12})_{1,\ldots\ldots,N}-t+(T_{22})_{1,\ldots\ldots,N}, \qquad (21a)$$

and for $i=2,\ldots,N$,

$$Y_i=-RF_v[t(T_{12})_{1,\ldots,i-1}+(T_{12})_{i,\ldots,N}]-t(T_{11})_{1,\ldots,i-1}$$
$$+(T_{22})_{i,\ldots,N}. \qquad (21b)$$

The cap layer interface elements of $\mathbf{d}$ can also be worked out in the following closed forms:

$$d\left(0,1,-\frac{d_1}{2};0,1,-\frac{d_1}{2}\right)=\frac{Y_1}{W}, \qquad (22)$$

$$d\left(-1,0,-\frac{d_0}{2};-1,0,-\frac{d_0}{2}\right)=\frac{Y_1F_0C_0+S_0\{(T_{21})_{1,\ldots,N}-RF_v[-t+(T_{11})_{1,\ldots,N}]\}}{W(F_0C_0+F_vS_0)},\tag{23}$$

$$d\left(-1,0,-\frac{d_0}{2};0,1,-\frac{d_1}{2}\right)=d\left(0,1,-\frac{d_1}{2};-1,0,-\frac{d_0}{2}\right)=\frac{Y_1F_0}{W(F_0C_0+F_vS_0)},\tag{24a}$$

and for $(n,i)\neq(0,1)$,

$$d\left(-1,0,-\frac{d_0}{2};n,i,-\frac{d_i}{2}\right)=\frac{Y_iF_0t^n}{W(F_0C_0+F_vS_0)}.\tag{24b}$$

From the knowledge of these interface matrix elements one can obtain the elements of the Green's function between any two points of the whole system [see Eq. (5)]. Here, we only give their expressions for two points belonging both either to the superlattice, or to the cap layer, or to the substrate:

(i) When the two points are inside the superlattice, $d(n,\,i,\,x_3,\,n';\,i',\,x_3')$ is given by Eq. (14) in which one has to replace $\mathbf{g}(M_m,\,M_{m'})$ by $\mathbf{d}(M_m,\,M_{m'})$ given by Eq. (19).

(ii) When the two points are inside the cap layer, $d(-1,\,0,\,x_3;\,-1,\,0,\,x_3')$ is given by Eq. (14) for $i=0$ and in which one has to replace $\mathbf{g}(M_m,\,M_{m'})$ by $\mathbf{d}(M_0,\,M_0)$, with $M_0\equiv(-1,0,\pm d_0/2)$.

The elements of this $(2\times2)$ matrix are given by Eqs. (22–24).

(iii) When the two points are inside the substrate

$$d(x_3,x_3')=-\frac{1}{2F_v}\,e^{-\alpha_v|x_3-x_3'|}+\left[d\left(-1,0,-\frac{d_0}{2};-1,0,-\frac{d_0}{2}\right)+\frac{1}{2F_v}\right]e^{-\alpha_v(x_3+x_3')},\tag{25}$$

where $d(-1,\,0,\,-d_0/2;\,-1,\,0,\,-d_0/2)$ is given by Eq. (23).

### B. Eigenfrequencies and eigenfunctions of the localized states

When the denominator of the Green's function $\mathbf{d}$ vanishes for a frequency lying inside the gaps of the infinite superlattice, one obtains localized states within the cap layer which decay exponentially inside the bulk of the superlattice. The explicit expression giving the frequency $\omega$ of these localized states is

$$W(\omega)=0,\tag{26a}$$

where $W(\omega)$ is given by Eq. (20), together with the condition

$$|(T_{22})_{1,\ldots,N}-RF_v(T_{12})_{1,\ldots,N}|>1.\tag{26b}$$

Condition (26b) ensures that the wave is decaying when penetrating into the superlattice far from the surface.

The eigenfunctions associated with these localized states are found to be

$$u(x_3)\propto Wd\left(-1,0,-\frac{d_0}{2};-1,0,-\frac{d_0}{2}\right)e^{\alpha_v x_3},\quad x_3\leqslant 0,\tag{27a}$$

$$u(x_3)\propto Wd\left(-1,0,-\frac{d_0}{2};-1,0,-\frac{d_0}{2}\right)\sinh\left[\alpha_0\left(\frac{d_0}{2}-x_3\right)\right]+Wd\left(-1,0,-\frac{d_0}{2};0,1,-\frac{d_1}{2}\right)\sinh\left[\alpha_0\left(\frac{d_0}{2}+x_3\right)\right],\quad -\frac{d_0}{2}\leqslant x_3\leqslant\frac{d_0}{2},\tag{27b}$$

$$u(n,i,x_3)\propto Wd\left(-1,0,-\frac{d_0}{2};n,i,-\frac{d_i}{2}\right)\sinh\left[\alpha_i\left(\frac{d_i}{2}-x_3\right)\right]+Wd\left(-1,0,-\frac{d_0}{2};n,i,\frac{d_i}{2}\right)\sinh\left[\alpha_i\left(\frac{d_i}{2}+x_3\right)\right],\quad -\frac{d_i}{2}\leqslant x_3\leqslant\frac{d_i}{2},\quad i=1,\ldots,N,\tag{27c}$$

where the Green's-function matrix elements defined by Eqs. (23)–(24) appear.

### C. The local densities of states

The local densities of states on the plane $(n,i,x_3)$ are given by

$$n(\omega^2,\mathbf{k}_\parallel;n,i,x_3)=-\frac{\rho_i}{\pi}\,\mathrm{Im}\,d^+(\omega^2,\mathbf{k}_\parallel;n,i,x_3;n,i,x_3),\tag{28}$$

where

$$d^+(\omega^2)=\lim_{\varepsilon\to0}d(\omega^2+i\varepsilon)\tag{29}$$

and $d(\omega^2)$ is the above-defined Green's function.

### D. The total density of states

The total density of states for a given value of $\mathbf{k}_\parallel$ is obtained by integrating over $x_3$ and summing on $n$ and $i$ the local density $n(\omega^2,\,\mathbf{k}_\parallel;\,n,\,i,\,x_3)$. A particularly interesting quantity is the density of states of the above-defined composite system from which the contributions of bulk substrate and bulk superlattice are substrated. This variation $\Delta n(\omega^2)$ can be written as

$$\Delta n(\omega^2)=\sum_{i=1}^{N}\Delta_i n(\omega^2)+n_0(\omega^2)+\Delta_v n(\omega^2),\tag{30}$$

where $\Delta_i n(\omega^2)$ is the variation of the density of states in any slab $i$, $n_0(\omega^2)$ the density of states in the cap layer, and $\Delta_v n(\omega^2)$ the variation of the density of states in the substrate. The explicit expressions for these quantities were found to be

$$\Delta_i n(\omega^2) = -\frac{\rho_i}{2\pi}\,\mathrm{Im}\,\frac{t}{(t^2-1)^2}\left(\frac{1}{\alpha_i S_i^2 W}\right)[(Y_i^2+Y_{i+1}^2)(C_iS_i-\alpha_i d_i)+2Y_iY_{i+1}(\alpha_i d_i C_i - S_i)],\quad i=1,\dots,N-1, \tag{31a}$$

$$\Delta_N n(\omega^2) = -\frac{\rho_N}{2\pi}\,\mathrm{Im}\,\frac{t}{(t^2-1)^2}\left(\frac{1}{\alpha_N S_N^2 W}\right)[(Y_N^2+(tY_1)^2)(C_NS_N-\alpha_N d_N)+2Y_NY_1 t(\alpha_N d_N C_N - S_N)], \tag{31b}$$

$$n_0(\omega^2) = -\frac{\rho_0}{2\pi}\,\mathrm{Im}\,\frac{Y_1}{W(T_{12})_{1,\dots\dots,N}}\left\{ d_0\left[(T_{12})_{1,\dots,N}+[(T_{11})_{1,\dots,N}-t]R\,\frac{F_v}{F_0^2}\right] + \frac{S_0F_0\left[(T_{12})_{1,\dots,N}-[(T_{11})_{1,\dots,N}-t]\,\frac{F_v}{F_0^2}\right]}{\alpha_0(F_0C_0+F_vS_0)}\right\}, \tag{32}$$

and

$$\Delta_v n(\omega^2) = -\frac{\rho_v}{\pi}\,\mathrm{Im}\,\frac{1}{2\alpha_v}\left\{\frac{1}{2F_v}+\frac{Y_1F_0C_0+S_0\{(T_{21})_{1,\dots,N}-RF_v[(T_{11})_{1,\dots,N}-t]\}}{W(F_0C_0+F_vS_0)}\right\}. \tag{33}$$

### E. The limit of a semi-infinite superlattice

(i) The case of a semi-infinite superlattice with a cap layer can be described from the above results, by making $F_v=0$ and $RF_v\rightarrow F_0S_0/C_0$. In particular, if the cap layer is of the same nature as the $N$th layer and of width $d_0<d_N$, we obtain from the above results [Eqs. (19)–(21) and (26)–(32)] the properties of a semi-infinite superlattice ending with an incomplete $i=N$ surface layer.

(ii) A semi-infinite superlattice ending with a complete $i=1$ surface layer is obtained from the above case (i) by taking the limit where the thickness $d_0$ of the cap layer goes to zero. This implies that $C_0$ is equal to 1 and $S_0$ vanishes. Equations (19)–(21) and (26)–(31) remain valid in this limit and provide all the physical results for such a semi-infinite superlattice. Let us be precise that in this limit $n_0(\omega^2)$ and $\Delta_v n(\omega^2)$ vanish.

### F. The limit of an interface between a semi-infinite superlattice and a homogeneous substrate

An interface between a semi-infinite superlattice and a homogeneous substrate is interesting by itself, in particular because specific localized and resonant modes may exist in its vicinity. Such a limit can be obtained from the above results given by Eqs. (19)–(33) by setting the width $d_0$ of the cap layer going to zero; this implies $S_0\rightarrow 0$, $C_0\rightarrow 1$, $R\rightarrow 1$, and $n_0(\omega^2)\rightarrow 0$.

## IV. APPLICATION TO A FOUR-LAYER SUPERLATTICE

### A. Analytical results

In order to illustrate the general results given before, we present here a simple and novel application to the special case of a four-layer superlattice. First, we show in this example how one calculates the unconventional sums appearing in the expressions defined by Eqs. (9):

$$\begin{aligned}(T_{11})_{1,\dots,4} = {}& C_4C_3C_2C_1 + C_2C_1S_4S_3\,\frac{F_3}{F_4} + C_3C_1S_4S_2\,\frac{F_2}{F_4}\\ &+ C_4C_1S_3S_2\,\frac{F_2}{F_3} + C_3C_2S_4S_1\,\frac{F_1}{F_4}\\ &+ C_4C_2S_3S_1\,\frac{F_1}{F_3} + C_4C_3S_2S_1\,\frac{F_1}{F_2}\\ &+ S_4S_3S_2S_1\,\frac{F_1}{F_2}\,\frac{F_3}{F_4},\end{aligned} \tag{34}$$

$$\begin{aligned}(T_{22})_{1,\dots,4} = {}& C_4C_3C_2C_1 + C_2C_1S_4S_3\,\frac{F_4}{F_3} + C_3C_1S_4S_2\,\frac{F_4}{F_2}\\ &+ C_4C_2S_3S_1\,\frac{F_3}{F_1} + C_4C_1S_3S_2\,\frac{F_3}{F_2}\\ &+ C_3C_2S_4S_1\,\frac{F_4}{F_1} + C_4C_3S_2S_1\,\frac{F_2}{F_1}\\ &+ S_4S_3S_2S_1\,\frac{F_2}{F_1}\,\frac{F_4}{F_3},\end{aligned} \tag{35}$$

$$\begin{aligned}(T_{21})_{1,\dots,4} = {}& C_4C_3C_2S_1F_1 + C_3C_2C_1S_4F_4 + C_4C_2C_1S_3F_3\\ &+ C_4C_3C_1S_2F_2 + C_4S_3S_2S_1\,\frac{F_1F_3}{F_2}\\ &+ C_2S_4S_3S_1\,\frac{F_1F_4}{F_3} + C_1S_4S_3S_2\,\frac{F_2F_4}{F_3}\\ &+ C_3S_4S_2S_1\,\frac{F_1F_4}{F_2},\end{aligned} \tag{36}$$

and

$$(T_{12})_{1,\ldots,4}=C_4C_3C_2S_1\,\frac{1}{F_1}+C_3C_2C_1S_4\,\frac{1}{F_4}+C_4C_2C_1S_3\,\frac{1}{F_3}+C_4C_3C_1S_2\,\frac{1}{F_2}+C_4S_3S_2S_1\,\frac{F_2}{F_1F_3}+C_3S_4S_2S_1\,\frac{F_2}{F_1F_4}+C_1S_4S_3S_2\,\frac{F_3}{F_2F_4}+C_2S_4S_3S_1\,\frac{F_3}{F_1F_4}. \tag{37}$$

With the help of these expressions, the dispersion relation of the surface modes [Eq. 20] becomes fully explicit. As a further illustration of the calculations of the local and total density of states [Eqs. (30)–(33)], we write down the quantities $Y_1$, $Y_2$, $Y_3$, $Y_4$ defined by Eqs. (21a) and (21b)

$$Y_1=-RF_v(T_{12})_{1,\ldots,4}-t+(T_{22})_{1,\ldots,4}, \tag{38}$$

$$Y_2=-RF_v\left[\frac{S_1}{F_1}\,t+C_4C_2\,\frac{S_3}{F_3}+C_4C_3\,\frac{S_2}{F_2}+C_3C_2\,\frac{S_4}{F_4}+S_4S_3S_2\,\frac{F_3}{F_4F_2}\right]-C_1t+\left(C_4C_3C_2+C_3S_4S_2\,\frac{F_4}{F_2}+C_2S_4S_3\,\frac{F_4}{F_3}+C_4S_3S_2\,\frac{F_3}{F_2}\right). \tag{39}$$

$$Y_3=-RF_v\left[\left(C_2\,\frac{S_1}{F_1}+C_1\,\frac{S_2}{F_2}\right)t+\left(C_4\,\frac{S_3}{F_3}+C_3\,\frac{S_4}{F_4}\right)\right]-\left(C_2C_1+S_2S_1\,\frac{F_1}{F_2}\right)t+C_4C_3+S_4S_3\,\frac{F_4}{F_3}, \tag{40}$$

and

$$Y_4=-RF_v\left[\left(C_3C_2\,\frac{S_1}{F_1}+C_3C_1\,\frac{S_2}{F_2}+C_2C_1\,\frac{S_3}{F_3}+S_3S_2S_1\,\frac{F_2}{F_1F_3}\right)t+\frac{S_4}{F_4}\right]-\left(C_3C_2C_1+C_3S_2S_1\,\frac{F_1}{F_2}+C_1S_3S_2\,\frac{F_2}{F_3}+C_2S_3S_1\,\frac{F_1}{F_3}\right)t+C_4. \tag{41}$$

## B. Numerical results

We now illustrate these theoretical results by a few numerical calculations for some specific examples. We report the results of dispersion relations, densities of states and eigenfunctions of surface acoustic phonons in a four-layer superlattice formed out of two different Nb slabs separated by two Cu slabs or by one Cu and one Fe slab. Table I gives the numerical values of the elastic constants, the mass densities, and the transverse speed of sound for these materials. The behavior of Rayleigh and Love waves on a Nb-Cu superlattice has been studied both experimentally[31–34] and theoretically.[35,36]

TABLE I. Elastic constants, mass densities and transverse speed of sound of Nb, Cu, and Fe.

| | $C_{44}$ ($10^{11}$ dyn/cm$^2$) | $\rho$ (g/cm$^3$) | $C_t$ ($10^5$ cm/s) |
|---|---|---|---|
| Nb | 28.7 | 8.57 | 1.83 |
| Cu | 75.3 | 8.92 | 2.905 |
| Fe | 118 | 7.8 | 3.89 |

We will show that increasing the number of the layers in each unit cell of the superlattice increases, in general the number of the minigaps and then the number of the surface modes. We also show that the creation from the infinite superlattice of a free surface gives rise to $\delta$ peaks of weight $(-\frac{1}{4})$ in the density of states, at the edges of any superlattice bulk band.[30] Then by considering together the two complementary semi-infinite superlattices obtained by cleavage of an infinite superlattice along a plane parallel to the interfaces, one always has as many localized surface modes as minigaps, for any value of $\mathbf{k}_\parallel$.

### 1. Semi-infinite superlattice in contact with vacuum

As a first example, we consider a Nb($d_1$)-Fe($d_2$)-Nb($d_3$)-Cu($d_4$) semi-infinite superlattice, where $d_i$ ($i=1$, 2, 3, and 4) represent the widths of the slabs forming the unit cell of the superlattice. $D=d_1+d_2+d_3+d_4$ is the period of the superlattice. Figure 2 gives the dispersion of bulk bands and surface modes as a function of $\mathbf{k}_\parallel D$, where $\mathbf{k}_\parallel$ is the propagation vector parallel to the interfaces, for $d_1=0.2D$, $d_2=d_4=0.35D$, and $d_3=0.1D$. We have pre-

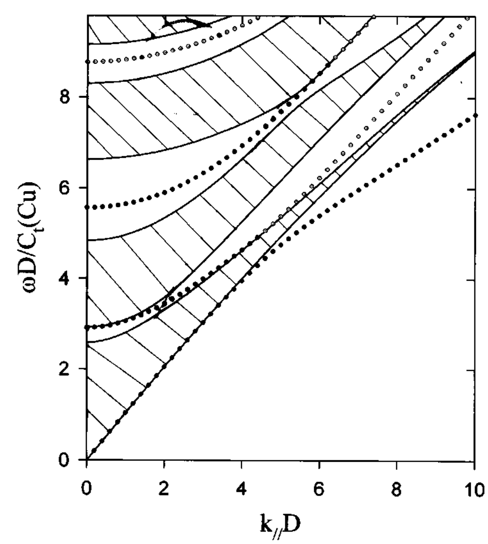


FIG. 2. Dispersion of bulk and surface transverse elastic waves in a semi-infinite Nb($d_1$)-Fe($d_2$)-Nb($d_3$)-Cu($d_4$) superlattice, with $d_1=0.2D$, $d_3=0.1D$, and $d_2=d_4=0.35D$, where $D=d_1+d_2+d_3+d_4$ is the period of the superlattice. The curves give $\omega D/C_t$(Cu) as a function of $k_\parallel D$, where $\omega$ is the frequency, $k_\parallel$ the propagation vector parallel to the interfaces, and $C_t$(Cu) the transverse speed of sound in Cu. The hatched areas represent the bulk bands. The filled circles represent the surface phonons for the semi-infinite superlattice terminated by a Nb layer of thickness $d_1$. The empty circles represent the surface phonons for the complementary superlattice terminated by a Cu layer of thickness $d_4$.

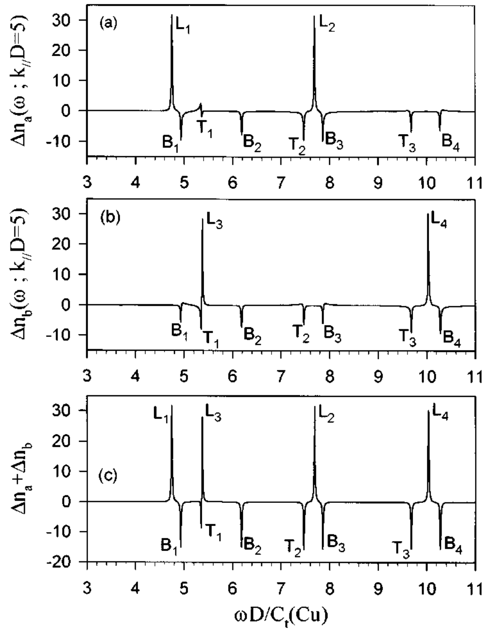


FIG. 3. (a) Variation in the density of states [in units of $D/C_t$(Cu)] between a semi-infinite Nb($d_1$)-Fe($d_2$)-Nb($d_3$)-Cu($d_4$) superlattice terminated by a Nb layer of thickness $d_1$ and the same amount of a bulk superlattice, as a function of $\omega D/C_t$(Cu), for $k_\parallel D=5$. $B_i$ and $T_i$, respectively, refer to $\delta$ peaks of weight $(-\frac{1}{4})$ situated at the bottom and the top of the bulk bands and $L_i$ indicates the localized surface modes. (b) Same as (a) but for the complementary superlattice terminated by a Cu layer of thickness $d_4$. (c) Same as (a) but for both complementary superlattices, $B_i$ and $T_i$, respectively, refer to $\delta$ peaks of weight $(-\frac{1}{2})$.

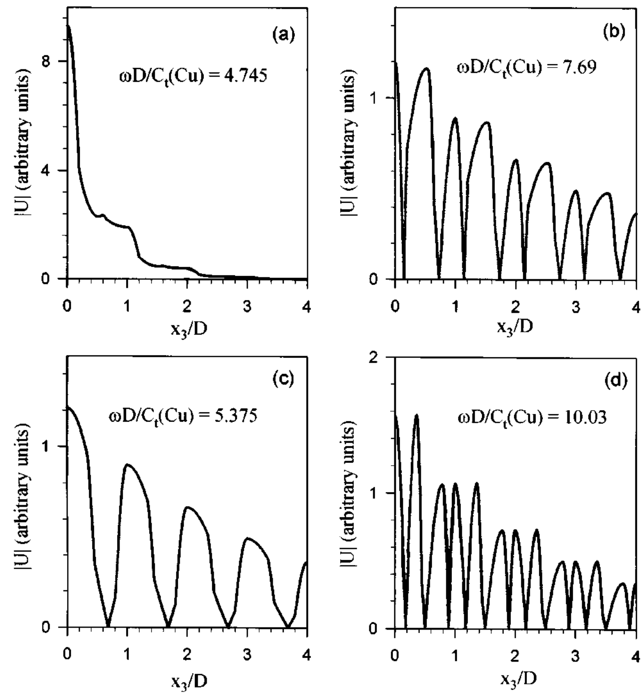


FIG. 4. Modulus of the displacement field versus depth for the surface waves occurring in Fig. 3 (i.e., for $k_\parallel D=5$) at reduced frequencies $[\omega D/C_t(\mathrm{Cu})]=4.745$ (a), $[\omega D/C_t(\mathrm{Cu})]=7.69$ (b), $[\omega D/C_t(\mathrm{Cu})]=5.375$ (c), and $[\omega D/C_t(\mathrm{Cu})]=10.03$ (d). The surface waves represented in Figs. (a) and (b) [respectively, (c) and (d)] are obtained when a Nb (respectively, a Cu) layer is at the surface of the semi-infinite superlattice [see Figs. 3(a) and 3(b)].

sented the surface modes of both complementary semi-infinite superlattices obtained by cleaving the infinite superlattice at the interface between a Nb layer of width $d_1$ and a Cu layer of width $d_4$. The hatched areas are the bulk bands separated by minigaps where the surface acoustic modes appear. We obtained a generalization of a result demonstrated analytically and numerically for two-layer superlattices by El Boudouti *et al.*[30] and observed experimentally for Al-Ag superlattices by Chen *et al.*,[37] namely, there are as many surface states as minigaps, each surface mode being associated with either one or the other of the complementary semi-infinite superlattices. One can also observe that the surface modes are very dependent on the type of crystal which is at the surface. On the other hand, there is a continuity between the surface branches of the two complementary superlattices when these branches reach a bulk band edge.

It can be shown analytically that the expression giving the frequencies of the surface modes for two complementary semi-infinite superlattices terminated by slabs of the same thickness as in the bulk is identical to the expression giving the standing waves of one unit cell with stress-free boundary conditions. This expression is given by $(T_{21})_{1,\ldots,4}=0$.

The variation in the vibrational density of states $\Delta n_a(\omega)$ [respectively, $\Delta n_b(\omega)$] between the semi-infinite superlattice terminated by a crystal of Nb of width $d_1=0.2D$ (respectively, Cu of width $d_4=0.35D$) and the same amount of the bulk superlattice was deduced from the calculation described in Secs. III F and IV A. These $\Delta n_a(\omega)$ and $\Delta n_b(\omega)$ are plotted in Figs. 3(a) and 3(b) for $\mathbf{k}_\parallel D=5$, as a function of the reduced frequency $[\omega D/C_t(\mathrm{Cu})]$. The $\delta$ functions appearing at the bulk band edges and at the frequencies of the surface modes are enlarged by the addition of a small imaginary part to the frequency $\omega$. The $\delta$ functions associated with the surface localized states are noted $L_i$ and the $\delta$ functions of weight $(-\frac{1}{4})$ situated, respectively, at the bottom and top of any bulk band are called $B_i$ and $T_i$. The form of these latter enlarged $\delta$ functions $B_i$ and $T_i$ are not exactly the same because of the contributions coming from the divergence in $(\omega-\omega_{B_i})^{-1/2}$ or $(\omega-\omega_{T_i})^{-1/2}$ ($\omega_{B_i}$ and $\omega_{T_i}$ are the frequencies of the bottom and the top of every bulk band of the superlattice), existing near the band edges in the densities of states in one dimension. Apart from the above $\delta$ peaks and the particular behavior near the band edges, the variation of the vibrational density of states does not show any other significant effect inside the bulk bands of the superlattice.

It is worth considering the variation in the density of states $\Delta n(\omega)$ between the two complementary semi-infinite superlattices, given in Figs. 3(a) and 3(b), and the initial infinite superlattice. Figure 3(c) gives the sum of the variations in the density of states of these complementary systems $\Delta n(\omega)=\Delta n_a(\omega)+\Delta n_b(\omega)$. This quantity is equal to zero for $\omega$ falling inside any superlattice bulk band. The loss of states due to the peaks of weight $(-\frac{1}{2})$ at every edge of the bulk bands is then compensated by the gain associated with the localized states ($L_1$, $L_2$, $L_3$, $L_4$) inside the minigaps in order to ensure the conservation of the total number of states.

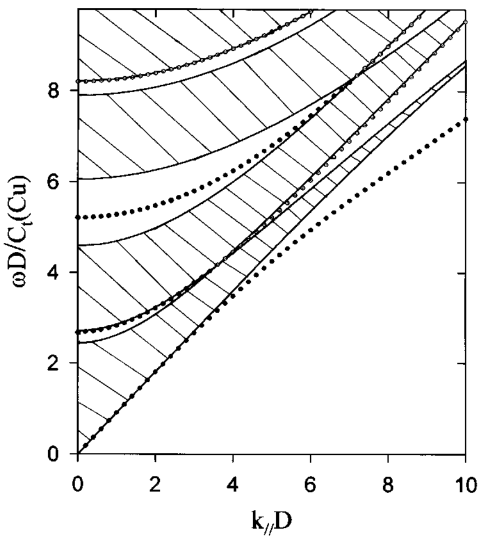


FIG. 5. Same as in Fig. 2 but for a semi-infinite Nb($d_1$)-Cu($d_2$)-Nb($d_3$)-Cu($d_4$) superlattice. The width of the slabs are the same as in Fig. 2. The filled circles represent the surface phonons for the semi-infinite superlattice terminated by a Nb layer of thickness $d_1$. The empty circles represent the surface phonons for the complementary superlattice terminated by a Cu layer of thickness $d_4$.

The behavior of surface modes displacement field as a function of the distance $x_3$ to the surface is sketched in Fig. 4, at the wave vector $\mathbf{k}_\parallel D=5$. Figures 4(a), 4(b), 4(c), and 4(d), respectively, refer to the surface modes labeled $L_1, L_2, L_3, L_4$ in Fig. 3 which occur at the following frequencies $[\omega D/C_t(\mathrm{Cu})]=4.745$, 7.69, 5.375, and 10.03. The parameter $t$ [Eq. (13)] which gives the attenuation of the surface wave from one period of the superlattice to the next when penetrating deep into the superlattice far from the surface takes, respectively, the values 0.205, 0.745, 0.74, and 0.828. Besides this exponential decrease of the envelope of the displacement field, one can also observe an increasing number of oscillations in each period of the superlattice when going to higher frequencies (let us notice that the frequencies of the modes $L_2$, $L_3$, $L_4$ fall inside the bulk bands of the constituent materials of the superlattice).

Now, in a second illustration, we assume that the Fe layers of width $d_2$ in the previous superlattice are replaced by Cu layers of the same width. Figure 5 gives the bulk bands and surface modes for the two complementary semi-infinite superlattices obtained in the same manner as in the previous example. The positions of surface modes are very different from those given in Fig. 2 even though the superlattices are terminated by the same layers at the surface.

One peculiarity of the example shown in Fig. 5 is the existence of successive bulk bands crossings; the crossing points are situated along a straight line defined as

$$\frac{\omega}{k_\parallel}=\left(\frac{C_{44}^2-C_{44}'^2}{\rho C_{44}-\rho' C_{44}'}\right)^{1/2}. \tag{42a}$$

This equation is obtained from the condition

$$F(\mathrm{Nb})=F(\mathrm{Cu}), \tag{42b}$$

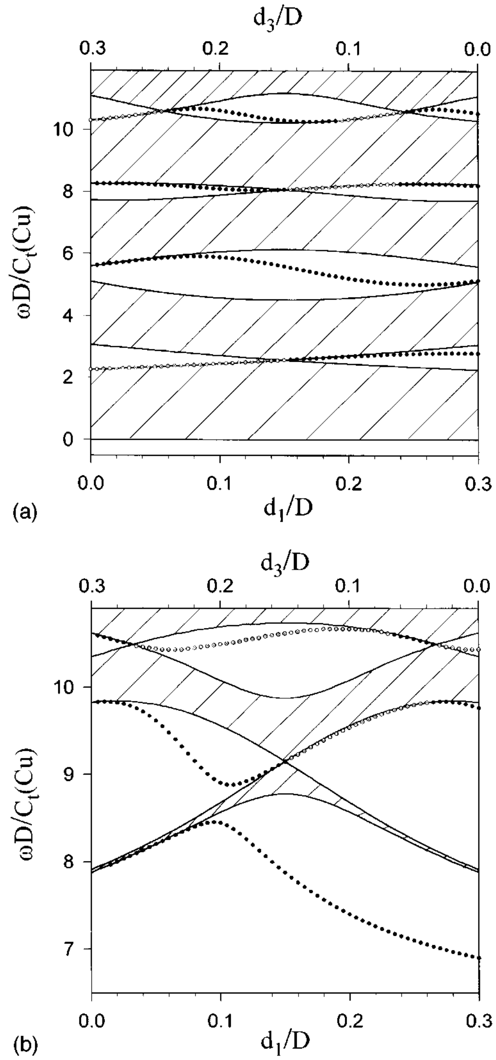


FIG. 6. Dispersion of bulk and surface transverse elastic waves in a semi-infinite Nb($d_1$)-Cu($d_2$)-Nb($d_3$)-Cu($d_4$) superlattice as a function of the thickness $d_1/D$ or $d_3/D$. The hatched areas represent the bulk bands. The filled circles represent the surface phonons for the semi-infinite superlattice terminated by a Nb layer of thickness $d_1$. The empty circles represent the surface phonons for the complementary superlattice terminated by a Cu layer of thickness $d_4$. (a) For $k_\parallel D=0$ and (b) for $k_\parallel D=10$.

where $F$ is defined in Eq. (3a). This is a sufficient condition for two bands to cross each other or, equivalently, a gap to close. The possibility of band crossing occurs if the slope of the straight line defined in Eq. (42a) is such that it cuts the bulk bands of the superlattice. Equation (42a) is actually valid for any $N$-layer superlattice composed of only two different materials. One can notice that the surfaces modes of one or the other of the complementary superlattices reach these crossing points and are in continuation of each other.

The number of the bulk bands and surface modes increases in general, with the number of the layers contained in each unit cell of the superlattice. Figure 6(a) [respectively, Fig. 6(b)] gives, for $k_\parallel D=0$ (respectively, for $k_\parallel D=10$), the dispersion of the bulk bands and surface modes as a function of the widths $d_1/D$ or $d_3/D$, the period of the superlattice being kept constant ($d_1/D$ increases from 0 to 0.3 when

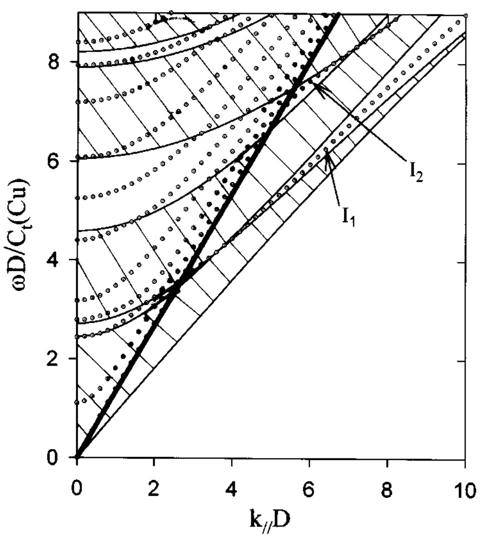


FIG. 7. Dispersion of localized and resonant modes induced by a Fe cap layer of thickness $d_0$, deposited on top of a semi-infinite Nb($d_1$)-Cu($d_2$)-Nb($d_3$)-Cu($d_4$) superlattice terminated by a full Nb layer of width $d_1$. The hatched areas represent the bulk bands. The heavy line indicates the bottom of the bulk band of Fe. The branches labeled ($I_i$) correspond to modes localized at the superlattice-cap layer interface.

$d_3/D$ decreases from 0.3 to 0). For $d_1/D = d_3/D = 0.15$, one finds the situation of a two-layer superlattice studied before by Camley *et al.*[36] For the other values of $d_1/D$, the number of the bulk bands and surface modes is multiplied by two as the number of the layers forming the unit cell is four instead of two. There are exceptions at some particular values of $d_1$ where two bulk bands cross each other and a gap disappears. The surface modes which are presented for both complementary semi-infinite superlattices reach the bulk band crossing points. One can also notice the continuity between surface modes corresponding to the complementary semi-infinite superlattices, both at the bulk bands crossing points and at the crossings of surface branches with the bulk band edges (see also Figs. 2 and 5).

#### 2. Capped semi-infinite superlattice in contact with vacuum

Now we assume that a cap layer of Fe, of thickness $d_0$, is deposited on top of the Nb($d_1$)-Cu($d_2$)-Nb($d_3$)-Cu($d_4$) semi-infinite superlattice terminated by a full Nb layer of width $d_1$, where $d_1 = 0.2D$, $d_2 = d_4 = 0.35D$, and $d_3 = 0.1D$. Figure 7 gives the dispersion of localized and resonant modes induced by a cap layer of width $d_0 = 4D$. These modes are obtained as well-defined peaks in the variation $\Delta n(\omega)$ (see Fig. 8) in the density of states between the capped superlattice and the same amount of the bulk superlattice without the cap layer (the calculation is explained in Secs. III D and IV A). It is worth noting that for another termination of the semi-infinite superlattice these modes will be quite different.

The localized and resonant modes induced by the cap layer can be divided in different groups according to the behavior of the corresponding eigenstates along the axis of the superlattice; they may propagate in both the superlattice and the cap layer, or propagate in one and decay in the other, or decay on both sides of the superlattice-cap layer interface.

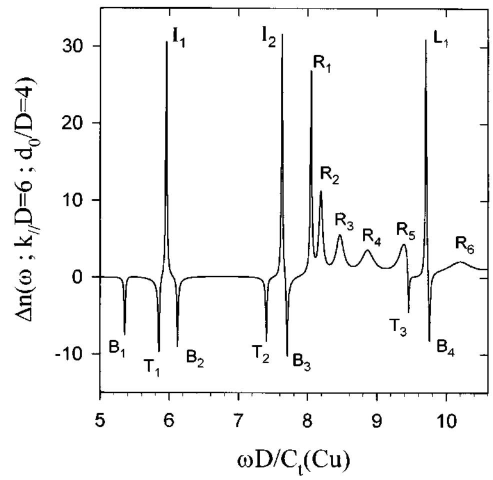


FIG. 8. Density of states [in units of $D/C_t$(Cu)] corresponding to the case described in Fig. 7, for $k_\parallel D = 6$. The contribution of the same amount of the bulk Nb($d_1$)-Cu($d_2$)-Nb($d_3$)-Cu($d_4$) superlattice was subtracted. $B_i$, $T_i$, and $L_i$ have the same meanings as in Fig. 3; $R_i$ and $I_i$ refer, respectively, to the resonant modes and to the localized modes at the superlattice-adlayer interface.

In the latter case, the modes (labeled $I_i$ in Figs. 7 and 8) are essentially localized states at the interface between the superlattice and the cap layer. The other modes are referred to as localized ($L_i$) if their envelope exponentially decays when penetrating deep into the superlattice, or as resonant modes ($R_i$) if they show an oscillatory behavior inside the superlattice. To illustrate these different types of behavior, we have plotted in Fig. 9(a), 9(b), and 9(c) the local densities of states as function of the space position $x_3$, for a given wave vector

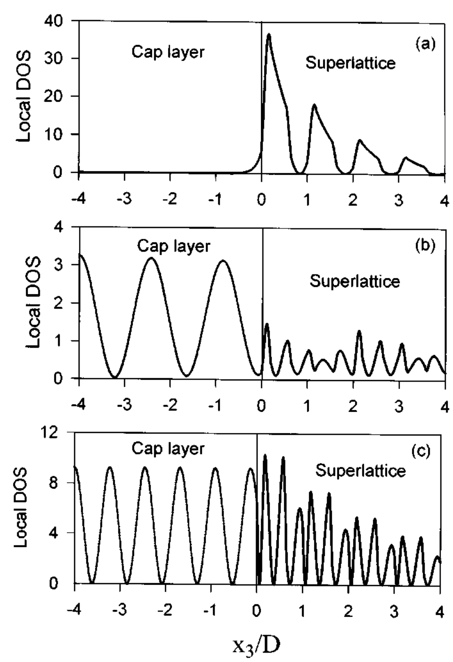


FIG. 9. (a) Spatial dependence of the local density of states (DOS) [in units of $D/C_t$(Cu)] corresponding to the case described in Fig. 7 at [$\omega D/C_t$(Cu)]=5.96 and $k_\parallel D = 6$. (b) The same as (a) but for [$\omega D/C_t$(Cu)]=8.565. (c) The same as (a) but for [$\omega D/C_t$(Cu)] =9.705.

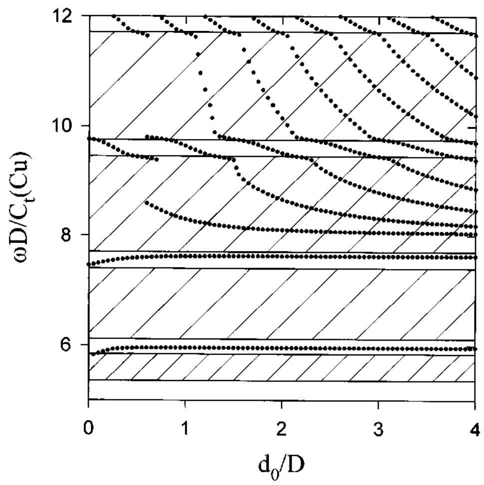


FIG. 10. Cap layer induced localized and resonant modes versus the width $d_0$ of the cap layer. The superlattice is the same as in Fig. 7 and $k_\parallel D=6$. The lowest two branches correspond to modes localized at the superlattice-cap layer interface.

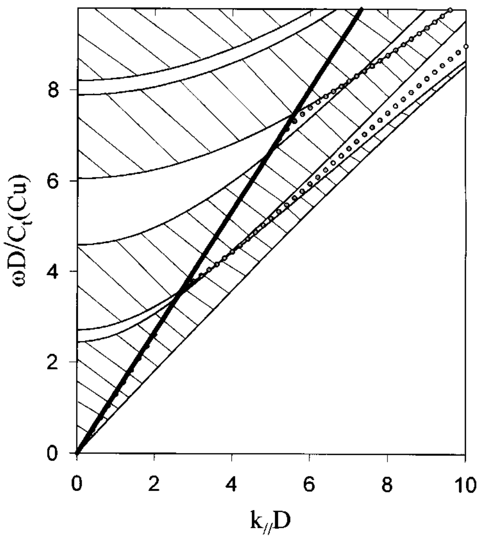


FIG. 11. Localized modes associated with the interface of the semi-infinite superlattice described in Fig. 7 and a Fe substrate. The heavy straight line indicates the bottom of the substrate bulk band.

$k_\parallel D=6$, and for different reduced frequencies $[\omega D/C_t(\mathrm{Cu})]=5.96$, 8.465, and 9.705 corresponding, respectively, to an interface mode $I_1$, a resonant mode $R_3$, and a localized mode $L_1$ in Fig. 8. This local density of states reflects the spatial behavior of the square modulus of the displacement field.

In the first case [Fig. 9(a)], the reduced frequency $[\omega D/C_t(\mathrm{Cu})=5.96]$ falls outside the cap layer and the superlattice bulk bands. The local density of states decays inside the cap layer and presents an oscillatory decay inside the superlattice. In the second case [Fig. 9(b)], the reduced frequency $[\omega D/C_t(\mathrm{Cu})=8.465]$ falls inside the bulk band of the superlattice. Consequently, the local density of states corresponding to this resonant mode presents an oscillatory behavior both inside the superlattice and inside the cap layer. However, the local density of states on average is more important inside the cap layer than in the superlattice. In the third case [Fig. 9(c)], the reduced frequency $[\omega D/C_t(\mathrm{Cu})=9.705]$ falls inside the gap of the superlattice. Now, the local density of states presents an oscillatory behavior in the space occupied by the cap layer and an oscillatory decay inside the superlattice.

The frequencies of the localized and resonant modes are very dependent upon the thickness $d_0$ of the cap layer as shown in Fig. 10, for $k_\parallel D=6$. The lowest two branches which correspond to cap layer-superlattice interface modes become almost independent of $d_0$ for $d_0 \geqslant 0.5D$. The next branches corresponding to resonant modes become closer to one another when $d_0$ increases, and as a consequence the intensities of the corresponding resonances increase. Let us also note that the curves in this figure becomes almost flat when a localized branch is going to become resonant by merging into a bulk band. The variation with $d_0$ is faster when the resonant branch penetrates deep into the band, but then the intensity of the resonant mode decreases, or may even vanish, in particular, when $d_0$ is small or the frequency is high. Finally, let us mention that for any given frequency $\omega$ in Fig. 10, there is a periodic repetition of the modes as a function of $d_0$.

When the thickness $d_0$ of the cap layer goes to infinite, we find the situation of a semi-infinite superlattice in contact with an homogeneous substrate. We address this case in the next section.

### *3. A semi-infinite superlattice in contact with a semi-infinite substrate*

To show the interface localized modes associated with the deposition of a semi-infinite superlattice on a semi-infinite substrate, we have chosen the same superlattice as in Sec. IV B 2 deposited on a substrate of Fe. Figure 11 gives the localized interface modes for the superlattice terminated by a full Nb layer of width $d_1$. One can remark that the frequencies of the interface modes in Figs. 7 and 11 are almost the same even though in the former case the substrate is replaced by a cap layer of finite thickness $d_0=4D$; moreover, the localization of the interface modes is similar in both cases. Let us also note that the frequencies of interface modes are very sensitive to the nature of the substrate and to the type of layer which is at the surface of the superlattice.

The variation $\Delta n_{11}(\omega)$ [respectively, $\Delta n_{12}(\omega)$] in the density of states between the semi-infinite superlattice terminated by a crystal of Nb of width $d_1=0.2D$ (respectively, Cu of width $d_4=0.35D$), in contact with a substrate of Fe and the same amount of the bulk superlattice and of the bulk homogeneous medium are plotted in Figs. 12(a) and 12(b) for $\mathbf{k}_\parallel D=1$, as a function of $\omega D/C_t(\mathrm{Cu})$. The $\delta$ functions of weight $(-\frac{1}{4})$ situated, respectively, at the bottom and top of any bulk band are called $B_i$ and $T_i$. $B_s$ refers to a $\delta$ peak of weight $(-\frac{1}{4})$ situated at the bottom of the substrate bulk band.

When one takes both complementary superlattices used in Figs. 12(a) and 12(b), the variation in the density of states $[\Delta n_1(\omega)=\Delta n_{11}(\omega)+\Delta n_{12}(\omega)]$ is shown to be equal to zero for frequencies $\omega$ belonging at the same time to the bulk bands of the substrate and the superlattice.[30] We have presented in Fig. 12(c) an example of this variation in the den-

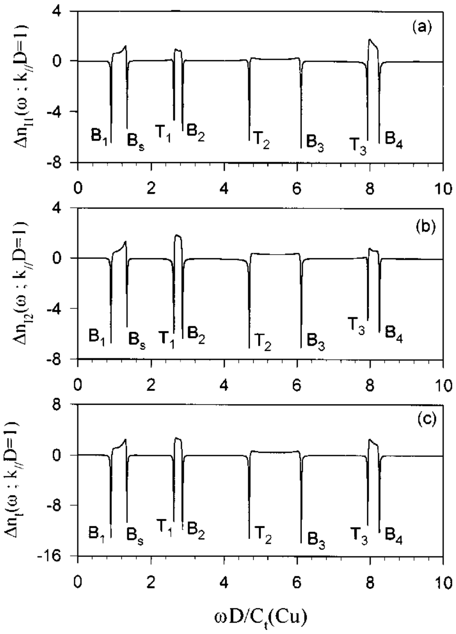


FIG. 12. (a) Variation in the density of states [in units of $D/C_t$(Cu)] at $k_{\parallel}D=1$, due to the creation of the superlattice-substrate interface. The superlattice is the same as in Fig. 7 and the substrate is Fe. $B_i$ and $T_i$ have the same meanings as in Fig. 3. $B_s$ refers to a $\delta$ peak of weight $(-\frac{1}{4})$ situated at the bottom of the substrate bulk band. (b) Same as (a) but for the complementary superlattice terminated by a Cu layer of thickness $d_4$. (c) Sum of the curves in (a) and (b).

sity of states for $\mathbf{k}_{\parallel}D=1$ for both complementary superlattices. Bearing in mind the loss of the $(-\frac{1}{2})$ state at the limits of any bulk band and the conservation of the total number of states, we are led to the necessary existence of positive contributions in the density of states lying inside the minigaps of the superlattice. The loss of states due to the peaks of weight $(-\frac{1}{2})$ at every edge of the bulk bands is compensated for by the gain associated with the positive contribution of $\Delta n_1(\omega)$ in the minigaps. This positive contribution is, however, differently partitioned between the two complementary superlattices.

## V. CONCLUSIONS

In this paper, we have presented an analytical calculation of the response function (Green's function) for acoustic waves of shear horizontal polarization in a semi-infinite $N$-layer superlattice, with or without a cap layer and in contact with an homogeneous substrate. These results are applicable to any $N$-layer superlattice system for which the elastic constants and the mass densities of the component crystals can be specified. These complete Green's function can be used for studying any vibrational property of the superlattice systems.[38,39] This includes the calculation of light-scattering spectra by acoustic phonons, the calculation of the eigenfunctions associated with the reflected and transmitted waves, the determination of the dispersion relations for surface (or interface) modes and their attenuation factors, and the calculation of the densities of states.

We focused our attention on the derivation of closed-form expressions for the local and total densities of states and the dispersion relation of bulk and surface or interface localized and resonant modes. One interest of the latter relations is that they are usable without a need of going into a detailed calculation.

Although these results are obtained for transverse elastic waves, they remain also valid for pure longitudinal waves propagating along the axis of the superlattice ($\mathbf{k}_{\parallel}=0$).

These surface dispersion modes may serve as a tool for the determination of elastic constants[33] of the materials from which the superlattice is built. Let us also mention that an extension of these studies to waves polarized in the sagittal plane will probably reveal even more interesting resonances.

Our general results are illustrated by a few applications to four-layer semi-infinite superlattices. We have shown that, in general, the number of minigaps and of surface states increases by increasing the number of layers in each unit cell. When two bulk bands cross each other, the surface states reach the crossing points in the $(\omega,k_{\parallel})$ plane. There is a continuation in this plane between the surface states of two complementary superlattices at the bulk band crossing points and more generally at a point where the surface states merge into a bulk band.

Another result of this paper was to generalize a previous theorem obtained in two-layer superlattices, namely, in creating two complementary semi-infinite superlattices from an infinite superlattice, one obtains as many localized surface states as minigaps for any value of $\mathbf{k}_{\parallel}$. This result is based on the general rule about the conservation of number of states and expresses a compensation between the losses of $\frac{1}{2}$ state at every bulk band edge (due to the creation of two free surfaces) and the gain due to the occurrence of surface states. In generalization of our previous studies in two-layer superlattices,[30] we presented in the last part of this paper a few illustrations of the different types of localized and resonant states due to the deposition of the cap layer on top of the superlattice, or associated with the interface between a semi-infinite superlattice and a substrate.

As a final remark, let us emphasize that the calculations presented here for the transverse elastic waves can be transposed straighforwardly to the electronic structure of superlattices in the effective-mass approximation,[8–10,40–42] or to the propagation of phonon or plasmon polaritons[8,35,43–46] in these heterostructures when each constituent is characterized by a local dielectric constant $\varepsilon(\omega)$. This is because both the equations of motion and the boundary conditions in the above problems involve similar mathematical equations. Therefore, the general behavior and conclusions obtained in this paper will prove to be useful for the two other physical problems.

## APPENDIX: TRANSFER-MATRIX METHOD FOR BULK AND SURFACE STATES

If one wants to obtain only the dispersion relations of bulk and surface localized states, it is convenient to use the classical transfer-matrix method, as done before for two-layer superlattices.[36–37,47] One writes first the displacement in the following form:

$$u(n,i,x_3)=(A_i e^{-\alpha_i x_3}+B_i e^{+\alpha_i x_3})e^{i(\mathbf{k}_\parallel\cdot\mathbf{x}_\parallel-\omega t)}e^{ik_3nD}. \tag{A1}$$

Using then the usual boundary conditions, one obtains easily the (2×2) matrix relations between $\binom{A_{i+1}}{B_{i+1}}$ and $\binom{A_i}{B_i}$ and then by transfer between $\binom{A_{N+1}}{B_{N+1}}$ and $\binom{A_1}{B_1}$. A particularly useful form of the transfer matrix is found then to be

$$T_{1,\ldots,N}=\Delta_N\Delta_{N-1}\ldots\ldots\Delta_2\Delta_1, \tag{A2}$$

where

$$\Delta_i=\begin{pmatrix} C_1 & \dfrac{S_i}{F_i} \\ F_iS_i & C_i \end{pmatrix}. \tag{A3}$$

The calculation of the four elements of $T_{1,\ldots,N}$ provides directly the Eqs. (9). Let us also note the useful property of the transfer matrix,

$$\det|\mathbf{T}|=(T_{11})_{1,\ldots,N}(T_{22})_{1,\ldots,N}-(T_{12})_{1,\ldots,N}(T_{21})_{1,\ldots,N}=1, \tag{A4}$$

valid for any number $N$ of layers from which the unit cell of the superlattice is built.

The derivation of the dispersion relation for bulk [Eqs. (10) and (11)], surface, and interface waves [Eqs. (20) and (26)] can then be done in the same manner as for two-layer superlattices.[36,37,47]


[1] K. K. Choi, B. F. Levine, G. G. Bethea, J. Walker, and R. J. Malik, Phys. Rev. Lett. **59**, 2459 (1987).
[2] H. Schneider, K. K. Kawashima, and K. Fujiwara, Phys. Rev. B **44**, 5943 (1991).
[3] D. F. Guo, W. C. Liu, W. S. Lour, C. Y. Sun, and R. C. Liu, J. Appl. Phys. **72**, 4414 (1992).
[4] L. Esaki, L. L. Chang, and E. E. Mendez, Jpn. J. Appl. Phys. **20**, L529 (1981).
[5] G. Bastard, Phys. Rev. B **25**, 7584 (1982).
[6] M. X. Jiang and J. Y. Lin, Phys. Rev. B **33**, 5851 (1986), Am. J. Phys. **55**, 462 (1987).
[7] H. Sakaki, M. Tsuychiya, and J. Yoshino, Appl. Phys. Lett. **47**, 285 (1985).
[8] B. Djafari-Rouhani and L. Dobrzynski, Solid State Commun. **62**, 609 (1987).
[9] L. Dobrzynski, Surf. Sci. **182**, 362 (1987); Phys. Rev. B **37**, 8027 (1988); Surf. Sci. **200**, 435 (1988); Surf. Sci. Rep. **11**, 139 (1990).
[10] P. F. Yuh and K. L. Wang, Phys. Rev. B **38**, 13 307 (1988).
[11] R. L. Liboff and S. R. Seidman, Phys. Rev. B **42**, 9552 (1990).
[12] S. Fafard, Y. H. Zhang, and J. L. Merz, Phys. Rev. B **48**, 12 308 (1993).
[13] J. J. Shi and S. H. Pan, Phys. Rev. B **48**, 8136 (1993).
[14] T. M. Kalotas, A. R. Lee, and A. K. Common, Phys. Status Solidi B **184**, 137 (1994).
[15] M. Nakayama, K. Kubota, S. Chika, H. Kato, and N. Sano, Solid State Commun. **58**, 475 (1986).
[16] P. V. Santos and L. Ley, Phys. Rev. B **36**, 3325 (1987).
[17] B. Jusserand, D. Paquet, F. Mollot, F. Alexandre, and G. Leroux, Phys. Rev. B **35**, 2808 (1987).
[18] D. J. Lockwood, R. L. S. Devine, A. Rodriguez, J. Mendialdua, B. Djafari-Rouhani, and L. Dobrzynski, Phys. Rev. B **47**, 13 553 (1993).
[19] J. Mendialdua, T. Szwacka, A. Rodriguez, and L. Dobrzynski, Phys. Rev. B **39**, 10 674 (1989).
[20] S. Tamura and J. P. Wolfe, Phys. Rev. B **38**, 5610 (1988); S. I. Tamura, *ibid*. **43**, 12 646 (1991).
[21] S. Mizuno and S. I. Tamura, Phys. Rev. B **45**, 13 423 (1992).
[22] R. Perez-Alvarez, F. Garcia-Moliner, and V. R. Velasco, J. Phys. Condens. Matter **7**, 2037 (1995).
[23] J. Mendialdua, A. Rodriguez, M. More, A. Akjouj, and L. Dobrzynski, Phys. Rev. B **50**, 14 605 (1994).
[24] B. L. Johnson and R. E. Camley, Phys. Rev. B **44**, 1225 (1991).
[25] S. A. Bulgakov and M. Nieto-Vesperinas, J. Opt. Soc. Am. A **13**, 500 (1996).
[26] J. Barnas, J. Phys. C **21**, 1021 (1988).
[27] R. Merlin, K. Bajema, R. Clarke, F. Y. Juang, and P. K. Bhattacharya, Phys. Rev. Lett. **55**, 1768 (1985); K. Bajema and R. Merlin, Phys. Rev. B **36**, 4555 (1987).
[28] D. J. Lockwood, A. H. Macdonald, G. C. Aers, M. W. C. Dharma-Wardana, R. L. S. Devine, and W. T. Moore, Phys. Rev. B **36**, 9286 (1987).
[29] M. W. C. Dharma-Wardana, A. H. Macdonald, D. J. Lockwood, J. M. Barideau, and D. C. Houghton, Phys. Rev. Lett. **58**, 1761 (1987).
[30] E. H. El Boudouti, B. Djafari-Rouhani, E. M. Khourdifi, and L. Dobrzynski, Phys. Rev. B **48**, 10 987 (1993).
[31] A. Kueny, M. Grimsditch, K. Miyano, I. Banerjee, C. Falco, and I. Schuller, Phys. Rev. Lett. **48**, 166 (1982).
[32] J. A. Bell, W. R. Benett, R. Zanoni, G. I. Stegeman, C. M. Falco, and C. T. Seaton, Solid State Commun. **64**, 1339 (1987).
[33] J. A. Bell, R. Zanoni, C. T. Seaton, G. I. Stageman, W. R. Benett, and C. M. Falco, Appl. Phys. Lett. **51**, 652 (1987).
[34] G. Carlotti, D. Fioretto, L. Palmieri, G. Socino, L. Verdini, Hua Xia, An Hu, and X. K. Zhang, Phys. Rev. B **46**, 12 777 (1992).
[35] A. Kueny and M. Grimsditch, Phys. Rev. B **26**, 4699 (1982).
[36] R. E. Camley, B. Djafari-Rouhani, L. Dobrzynski, and A. A. Maradudin, Phys. Rev. B **27**, 7318 (1983).
[37] W. Chen, Y. Lu, H. J. Maris, and G. Xiao, Phys. Rev. B **50**, 14 506 (1994).
[38] M. G. Cottam and A. A. Maradudin, in *Surface Excitations*, Modern Problems in Condensed Matter Sciences (North-Holland, Amsterdam 1984), Vol. 9.
[39] M. Babiker, N. C. Constantinou, and M. G. Cottam, J. Phys. C **20**, 5481 (1987).
[40] Hung-Sik Cho and P. R. Pruncal, Phys. Rev. B **36**, 3237 (1987).
[41] M. Steslicka, R. Kucharczyk, and M. L. Glasser, Phys. Rev. B **42**, 1458 (1990).

[42] M. Steslicka, R. Kucharczyk, E. H. El Boudouti, B. Djarfari-Rouhani. M. L. Bah, A. Akjouj, and L. Dobrzynski, Vacuum **46**, 621 (1995).
[43] M. L. Bah, A. Akjouj, and L. Dobrzynski, Surf. Sci. Rep. **16**, 95 (1992).
[44] A. Dereux, J. P. Vigneron, P. Lambin, and A. A. Lucas, Phys. Rev. B **38**, 5438 (1988); Phys. Scr. **38**, 462 (1988).
[45] J. J. Quinn, G. Eliasson, and P. Hawrylak, *Spatial Dispersion in Solids and Plasmons*, edited by P. Halevi (North-Holland, Amsterdam, 1992), Vol. 1, Chap 4, p.243.
[46] M. L. Bah, A. Akjouj, E. H. El Boudouti, B. Djafari-Rouhani, and L. Dobrzynski, J. Phys. Condens. Matter **8**, 4171 (1996).
[47] E. M. Khourdifi and B. Djafari-Rouhani, Surf. Sci. **211/212**, 361 (1989).